

## Interleaved Landsman Converter with Class Topper Optimized PI Control in Sensorless BLDC Motor Drive for Electric Vehicle

<sup>1</sup>Suresh V., <sup>1</sup>Kishore R.D., <sup>2</sup>Jahnavi V.G., <sup>1</sup>Manjula D., <sup>2</sup>Lokesh M.

<sup>1</sup>Department of Electrical & Electronics Engineering, Godavari Global University, Rajahmundry, India.

<sup>2</sup>Department of Electrical & Electronics Engineering, Godavari Institute of Engineering and Technology, Rajahmundry, India.

**Abstract.** The main objectives of the study are to develop a brushless direct current (BLDC) motor drive system with enhanced efficiency, reliability, and cost-effectiveness for electric vehicle (EV) applications. The proposed system integrates an advanced interleaved Landsman converter and an optimized Proportional-Integral (PI) controller for efficient energy management and motor control. In order to achieve the set goals, the following tasks were accomplished: The scientific novelty of this work lies in the design of a novel interleaved Landsman converter along with Class Topper Optimization (CTO) algorithm. The converter is designed to optimize power conversion from photovoltaic (PV) sources to the energy required for the BLDC motor; the algorithm is implemented to hyper-tune the PI controller for precise and rapid response; a bidirectional converter was employed to manage the charging and discharging of the battery system, ensuring adequate power distribution during peak demands; and a single-phase voltage source inverter (VSI) was utilized for DC-AC conversion to drive the BLDC motor. The system was tested in MATLAB/Simulink to evaluate its performance. The most important results are the achievement of high voltage conversion efficiency of 97.42%, a minimized settling time of 0.1 seconds, and rapid convergence speed, which collectively demonstrate the system's ability to provide reliable and efficient operation for EV propulsion. The significance of obtained results is the potential to revolutionize EV motor drive systems by offering an innovative, highly efficient, and scalable solution. This system not only enhances energy utilization and motor performance but also supports the widespread adoption of sustainable EV technology.

**Keywords:** electric vehicles, BLDC motor, interleaved Landsman converter, Class Topper optimization, voltage source inverter, PI controller.

DOI: <https://doi.org/10.52254/1857-0070.2025.1-65.14>

UDC: 621.362

### Convertor Landsman intercalat cu control PI optimizat Class Topper în motorul BLDC fără senzori pentru vehicule electrice

<sup>1</sup>Suresh V., <sup>1</sup>Kishore R.D., <sup>2</sup>Jahnavi V.G., <sup>1</sup>Manjula D., <sup>2</sup>Lokesh M.

<sup>1</sup>Universitatea Globală Godavari, Rajahmundry, India

<sup>2</sup> Institutul de Inginerie și Tehnologie Godavari, Rajahmundry, India.

**Abstract.** Obiectivele principale ale studiului sunt dezvoltarea unui sistem de acționare cu motor fără perii de curent continuu (BLDC) cu eficiență, fiabilitate și rentabilitate îmbunătățite pentru aplicațiile vehiculelor electrice (EV). Sistemul propus integrează un convertor Landsman intercalat avansat și un controler Proporțional-Integral (PI) optimizat pentru gestionarea eficientă a energiei și controlul motorului. Pentru a atinge obiectivele stabilite, au fost îndeplinite următoarele sarcini: Noutatea științifică a acestei lucrări constă în proiectarea unui nou convertor Landsman intercalat împreună cu algoritmul Class Topper Optimization (CTO). Convertorul este proiectat pentru a optimiza conversia puterii de la sursele fotovoltaice (PV) la energia necesară pentru motorul BLDC; algoritmul este implementat pentru a regla hipercontrolerul PI pentru un răspuns precis și rapid; a fost folosit un convertor bidirecțional pentru a gestiona încărcarea și descărcarea sistemului de baterii, asigurând o distribuție adecvată a energiei în timpul solicitărilor de vârf; și un inverter de sursă de tensiune monofazat (VSI) a fost utilizat pentru conversia DC-AC pentru a conduce motorul BLDC. Sistemul a fost testat în MATLAB/Simulink pentru a-și evalua performanța. Cele mai importante rezultate sunt obținerea unei eficiențe de conversie de înaltă tensiune de 97,42%, un timp de așezare minim de 0,1 secunde și viteza de convergență rapidă, care demonstrează în mod colectiv capacitatea sistemului de a oferi o funcționare fiabilă și eficientă pentru propulsia EV. Semnificația rezultatelor obținute este potențialul de a revoluționa sistemele de acționare a motoarelor EV, oferind o soluție inovatoare, extrem de eficientă și scalabilă. Acest sistem nu numai că îmbunătățește utilizarea energiei și performanța motorului, dar susține și adoptarea pe scară largă a tehnologiei EV sustenabile.

© Suresh V., Kishore R.D., Jahnavi G.V., Manjula D., Lokesh M. 2025

**Cuvinte-cheie:** vehicule electrice, motor BLDC, convertor interleaved Landsman, CTO, VSI, controler PI.

**Преобразователь Landsman с чередованием фаз и оптимизированным ПИ-регулятором класса Torrer в бессенсорном приводе двигателя BLDC для электромобиля**

**<sup>1</sup>Суреш В., <sup>1</sup>Кишоре Р.Д., <sup>2</sup>Жахнави В.Г., <sup>2</sup>Манжула Д., <sup>2</sup>Локеш М.**

<sup>1</sup>Godavari Global University, Раджамандри

<sup>2</sup>Godavari Institute of Engineering and Technology

Раджамандри, Индия

**Аннотация.** Основными целями исследования являются разработка системы привода бесщеточного двигателя постоянного тока (BLDC) с повышенной эффективностью, надежностью и экономической эффективностью для применения в электромобилях (EV). Предлагаемая система объединяет усовершенствованный преобразователь Landsman с чередованием и оптимизированный пропорционально-интегральный (ПИ) контроллер для эффективного управления энергией и управления двигателем. Для достижения поставленных целей были выполнены следующие задачи: Научная новизна этой работы заключается в разработке нового преобразователя Landsman с чередованием вместе с алгоритмом оптимизации класса Torrer (СТО). Преобразователь предназначен для оптимизации преобразования энергии от фотоэлектрических (PV) источников в энергию, необходимую для двигателя BLDC; алгоритм реализован для гипернастройки ПИ-контроллера для точного и быстрого реагирования; двунаправленный преобразователь использовался для управления зарядкой и разрядкой системы аккумуляторных батарей, обеспечивая адекватное распределение мощности во время пиковых нагрузок; а однофазный инвертор напряжения (VSI) использовался для преобразования постоянного тока в переменный для управления двигателем BLDC. Система была протестирована в MATLAB/Simulink для оценки ее производительности. Наиболее важными результатами являются достижение высокой эффективности преобразования напряжения 97,42%, минимизированное время установления 0,1 секунды и высокая скорость сходимости, которые в совокупности демонстрируют способность системы обеспечивать надежную и эффективную работу для движения электромобилей. Значимость полученных результатов заключается в потенциале революционизировать системы привода электромобилей, предлагая инновационное, высокоэффективное и масштабируемое решение. Эта система не только повышает использование энергии и производительность двигателя, но и поддерживает широкое внедрение устойчивой технологии электромобилей.

**Ключевые слова:** электромобили, двигатель BLDC, преобразователь Interleaved Landsman, CTO, VSI, ПИ-регулятор.

## I. INTRODUCTION

As of right now, 16.2% of the world's greenhouse gas emissions come from the transportation sector, which is mostly dependent on Internal Combustion Engine (ICE)-based automobiles [1-2]. Thus, EVs are becoming advanced for diminishing tailpipe emissions, noise pollution and maintenance costs compare to ICE vehicles [3]. In EVs, the usage of BLDC motor is desirable because of its high dependability, efficiency, low noise rate, longer operation [4-5]. When motor driven EVs are fuelled by a significant percentage of Renewable Energy Sources (RES), minimize the global warming issues by generating cleaner energy[6-7]. Among various RES, Solar powered BLDC motor driven EVs attains environmental advantages over minimized reliance on fossil fuels [8]. Nevertheless, since PV has a minimum output voltage, DC-DC converters are essential to provide an enhanced and stable voltage output [9]. A converter in [10] provides boost up voltage at high duty ratios at the expense of efficacy, due to its conduction losses it is unable to provide higher voltage gain [10]. Cuk converter in [11] have

continuous output and input currents, but they also have minimal voltage gains and efficiency. The characteristics of a Single-Ended Primary-Inductance Converter (SEPIC) in [12] attains higher voltage conversion ratios, despite it has maximize current ripples. In order to attain high step-up voltage gain and lessen the voltage stress on switches, the converters introduced in [13] incorporate the interleaved parallel boost converter with switched-capacitor and linked inductor module, however their output current is not constant and much voltage gain is unable to attain [14]. Henceforth, The Interleaved Landsman converter is designed for BLDC motor driven EV to achieve low output ripple voltage, high efficiency as well as high power density. Despite this, the control performance is desirable for stabilizing the output of converter [15], thus conventional Optimization approaches are utilized as shown in Table 1 with its benefits and challenges.

The recently employed optimization approaches comes with major advantages as well as drawbacks, thus the proposed work utilized a

Class Topper Optimization approach by the goal of overcoming the drawbacks faced by the above

discussed approaches with minimized settling time and convergence speed.

Table 1

Overview of Traditional Optimization Topologies

| Optimization Methodologies            | Advantages  | Drawbacks  |
|---------------------------------------|---|--|
| Genetic Alogrithm (GA) [16]           | It has high performance in settling time            | Poor convergence speed   |
| Particle Swarm Optimization [17]      | It convergence quickly                              | It has high overshoot problems                                     |
| FireFly Algorithm (FFA) [18]          | It stabilize the output with minimized oscillations | Firefly affects from complexity, computational and time            |
| Black Widow Optimizer (BWO) [19]      | It minimizes the overshoot issues.                  | It unable to avoid local optima and has a slow rate of convergence |
| Jellyfish Search Optimizer (JSO) [20] | The complexity and convergence speed is improved.   | The settling time is high  |

Subsequently, following points shows a foremost contributions of the proposed approach,

- ✓ Incorporating a novel Interleaved Landsman converter for efficient power conversion, specifically to handle PV energy source.
- ✓ Implementing Class Topper Optimized PI controller improvizes the stable performance for designed converter by exhibiting minimized settling time and improved convergence speed.
- ✓ Integrating battery with bidirectional converter allows bidirectional flow of power by ensuring charging and discharging process of battery.
- ✓ Employing PI controller for efficient BLDC motor control, which safeguards the motor operation at desired speed.

- ✓ Overall, the proposed concept integrates innovative energy management and motor control by addressing the needs of EV propulsion. By combining PV source with EV motor, a sustainable energy solution is promoted in transportation.

## II. PROPOSED SYSTEM MODELLING

When developing EVs, the two main factors to consider are efficiency and cost. Because of its high efficiency, high flux density per unit space, and minimal maintenance requirements, BLDC motors are being used in these applications more and more. Moreover, to supply energy with sustainable solutions are crucial, hence the proposed study develops a novel converter with optimized technique as shown in Fig. 1 for providing sustainable power supply.

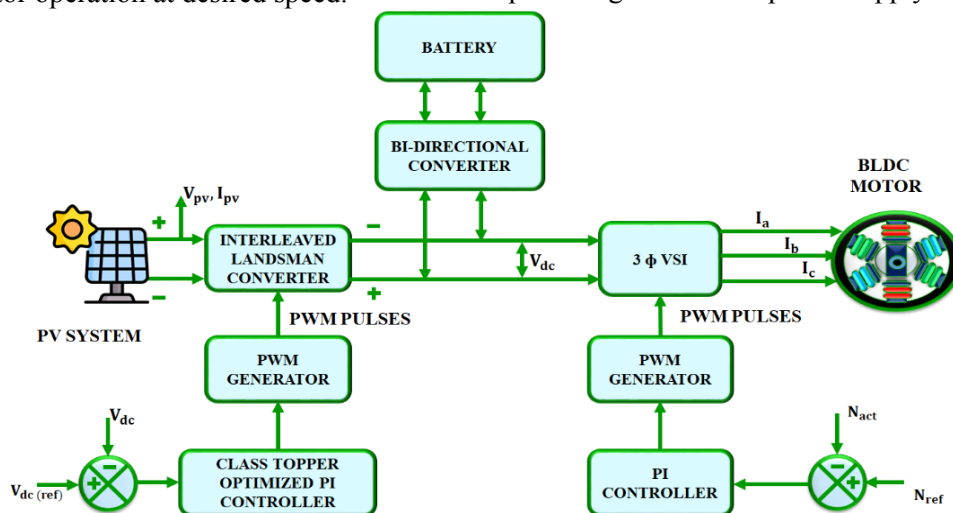
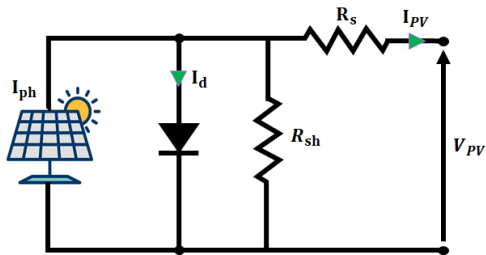


Fig. 1. Block diagram of PV based BLDC motor fed EV.

The supply of low output PV is fed to Interleaved Landsman converter for stepping up into the require level of BLDC motor and to stabilize the output of converter, it is given to CTO-PI controller. Moreover, the pulses for the switching operation of developed converter is obtained by PWM genertor, consequently, boosted and stabilized output in DC link is deliver to three phase for DC-AC conversion process. The signals  $V_{dc(ref)}$  denotes the pre-defined setpoint for the desired voltage whereas  $V_{dc}$  is the real-time DC link voltage measured at the converter output using the voltage sensor. Also,  $N_{ref}$  represents the desired speed of the BLDC motor and  $N_{act}$  is the real-time speed of the BLDC motor measured using a speed sensor. Additionally, the speed of BLDC motor is efficiently regulated by comparing the reference speed with acutal, which generates error signal and gets compensated with the assistance of PI controller. On the other hand, battery system is incorporated for storing additional energy when PV module generates excess power and it supply power back to BLDC motor during absence of PV. For managing charging and discharging process of battery, the bidirectional converter is utilized. Thereby, BLDC motor driven EV gets continous power supply with higher performance.

*A. Modelling of PV system*

The PV module is employed for generating clean energy by absorbing sunlight and convert into usable electricity, which is highly suitable for BLDC motor driven EV. Mostly, single diode model of PV is used as represents in Fig. 2, which consists of parallel diode, photo current source, shunt and series resistors correspondingly.



**Fig. 2. Circuit of single diode PV array.**

In the above figure,  $I_{ph}$ -photocurrent,  $I_d$ -diode current,  $R_s$ -series resistance,  $R_{sh}$ -shunt resistance,  $I_{PV}$ -output current,  $V_{PV}$ -output voltage,  $R_L$ - load resistance. The arithmetical model of Fig. 2 is defined by the following equation (1),

$$I_{pv} = I_{ph} - I_d - I_r = I_{ph} - I_o \left( e^{\frac{V_{pv} + R_{s1} PV}{nV_t}} - 1 \right) \dots \dots - \frac{V_{pv} + R_{s1} PV}{R_{sh}} \quad (1)$$

Here,  $I_{PV}$ - output current,  $I_{ph}$ -photocurrent,  $I_d$ -diode reverse saturation current,  $I_o$ -output voltage across PV cell,  $n$ -ideality factor,  $R_s, R_{sh}$ -series and shunt resistance,  $I_r$ -current across shunt resistance, the term  $V_t$  denotes the thermal voltage and is given by the below equation,

$$V_t = \frac{kT}{q} \quad (2)$$

Where,  $T$  specifies absolute temperature,  $q$  indicates electronic charge and  $k$  denotes Boltzmann constant.

In this context, the output of PV varies under changing weather conditions, thus to stepup into the required energy for BLDC motor fed EV, the proposed work introduces a novel Interleaved Landsman converter, which has the capacity of boosting the lower output into higher level with better efficiency and minimized losses as elaborated below.

*B. Modelling of Interleaved Landsman Converter*

The Interleaved Landsman converter emerges a promising solution for boosting the output voltage from PV array for optimizing the performance of BLDC motor driven Evs. The interleaving technique as represented in Fig. 3 helps to minimize the current ripples on the input side and voltage ripple on output side. It performs 2 operating modes as shown in Fig. 4 followed by switching waveform in Fig. 5.

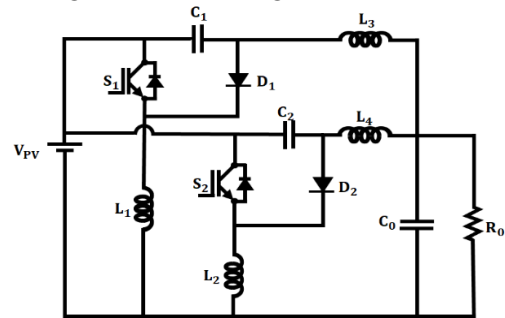


**Fig. 3. Circuit diagram of designed interleaved Landsman converter.**

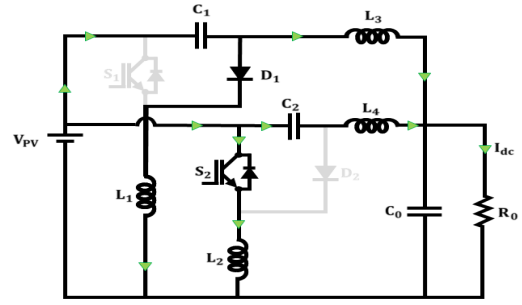
**Mode 1:** In this state, switch  $S_1$  is ON and  $S_2$  is in OFF condition, while diode  $D_1$  is OFF and  $D_2$  is ON. The inductors  $L_1$  and  $L_3$  are charging as current flows through it. Simulatenously,  $L_2$

and  $L_4$  are discharging and the load gets supply by the capacitor  $C_1$ , while capacitor  $C_2$  gets charge from the inductor current.

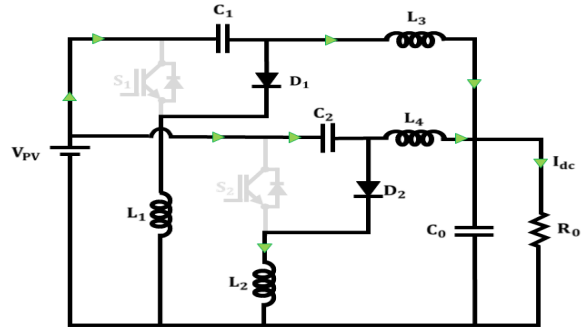
**Mode 2:** Both switches  $S_1$  and  $S_2$  are in magnetized state, while both diodes are in non conduction  $L_1, L_2, L_3, L_4$  mode, during this phase all the inductors are charging as the switches allows current flow directly over the inductors. Subsequently, the  $C_1$  capacitors and  $C_2$  discharges energy to the load as signified in Fig. 4(b).

**Mode 3:** In this phase,  $S_1$  is in non-conduction mode, while  $S_2$  in ON state, in this, the inductors  $L_1$  and  $L_3$  continue charging, while the  $L_2$  and  $L_4$  are discharging. In this mode,  $D_2$  is OFF, preventing current from flowing through that path. Capacitor  $C_1$  begins to charge from the energy released by the discharging inductors, while capacitor  $C_2$  discharges to power the load.

**Mode 4:** In the Final Mode, both switches  $S_1$  and  $S_2$  are in OFF state and all the inductors releases its charged energy. Meanwhile, capacitors  $C_1$  and  $C_2$  are charging as its receive energy from the discharging inductors. Diodes  $D_1$  and  $D_2$  are in ON condition, allowing current flow to flow through the converter to continue powering the load.

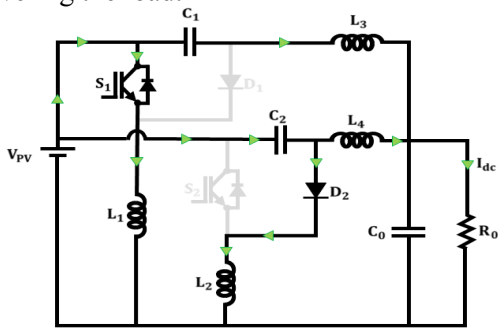


(c)

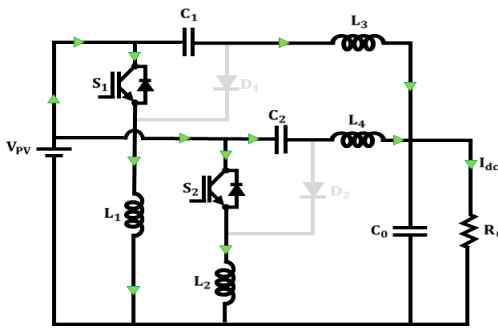


(d)

**Fig. 4. Modes of operation for developed interleaved Landsman converter.**



(a)



(b)

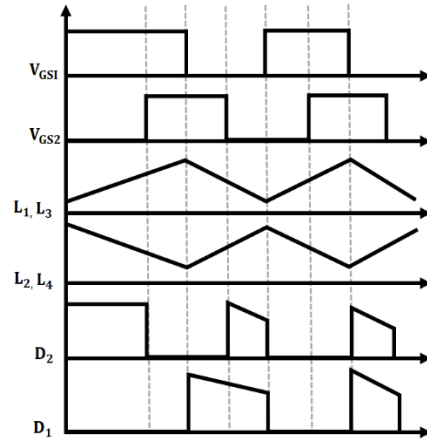


**Fig. 5. Timing waveform of developed converter**

$$\Delta IL_1 = \frac{\Delta \phi}{L_1} = \frac{1}{L_1} \frac{1}{2} \frac{\Delta V_{C1}}{2} \frac{T}{2} \quad (3)$$

$$\Delta IL_2 = \frac{\Delta \phi}{L_2} = \frac{1}{L_2} \frac{1}{2} \frac{\Delta V_{C2}}{2} \frac{T}{2} \quad (4)$$

Here,  $\Delta IL_1, \Delta IL_2$ -current ripple in  $L_1$  and  $L_2$ ,  $\Delta \Phi$  -change in magnetic flux through inductor,  $\Delta V_{C1}, \Delta V_{C2}$ -voltage ripple across  $C_1$  and  $C_2$ . The current flowing over  $C_1$  is calculated as,

$$i_{C1} = I_{L1} = C_1 \frac{\Delta V_{C1}}{(1-D)T} \quad (5)$$

$$i_{c_2} = I_{L_2} = C_2 \frac{\Delta V_{C_2}}{(1-D)T} \quad (6)$$

Here,  $T$  denotes the switching period and  $D$  specifies the duty ratio and from the equation (5 and 6), the voltage ripple content in  $V_{C_1}$  and  $V_{C_2}$  is calculated as,

$$\Delta V_{C_1} = \frac{1L_1}{C_1}(1-D)T \quad (7)$$

$$\Delta V_{C_2} = \frac{1L_2}{C_2}(1-D)T \quad (8)$$

Thus, the following equation (9 and 10) derives by substituting the equations (7-8) into (3-4),

$$\Delta IL_2 = \frac{1}{L_2} \frac{1}{2} \frac{I_{L_2}}{C_2} (1-D)T \frac{T}{2} \quad (9)$$

$$\Delta IL_1 = \frac{1}{8L_1C_1} \frac{I_{L_1}(1-D)}{f^2sw} \quad (10)$$

$$\Delta IL_2 = \frac{1}{8L_2C_2} \frac{I_{L_2}(1-D)}{f^2sw} \quad (11)$$

The above equation is standardised as,

$$\frac{\Delta IL_1}{IL_1} = \frac{1}{8L_1C_1} \frac{(1-D)}{f^2sw} \quad (12)$$

$$\frac{\Delta IL_2}{IL_2} = \frac{1}{8L_2C_2} \frac{(1-D)}{f^2sw} \quad (13)$$

Here,  $f_{sw} = \frac{1}{T}$  denotes the switching frequency, Following equation shows the relationship over the input and output,

$$IL_1 = \frac{D}{1-D} I_{dc} \quad (14)$$

$$IL_2 = \frac{D}{1-D} I_{dc} \quad (15)$$

The output current of Interleaved landsman converter is stated as  $I_{dc}$  thus the value of  $IL_1$  and  $IL_2$  is substitute into equation (11 and 12), which gives

$$L_1 = \frac{DI_{dc}}{8f^2swC_1\Delta IL_1} \quad (16)$$

$$L_2 = \frac{DI_{dc}}{8f^2swC_2\Delta IL_2} \quad (17)$$

With the aid of developed Interleaved converter, the satisfactory power supply for BLDC motor is efficiently delivered. Even though, the PI controller plays a significant role for stabilizing the output energy from the converter, it has to be effectively tuned with the aid of optimization topology for attaining better performance, thus the class topper optimization is established in this study as described below.

### C. Modelling of Class Topper Optimized PI Controller

The motivation behind the class topper optimisation method comes from the school, where students' learning behaviours are evaluated based on their knowledge in a class, and they compete with one another to become the class topper. The student who ranks highest in the class is regarded as the most knowledgeable member of the group. A meta heuristic population-based approach is used in the class topper optimisation process. This algorithm achieves global optima improvement through student learning at every level.

**Class level:** The student with the greatest knowledge in the class is chosen from within the section, and section toppers compete for the title of class topper. Meanwhile class toppers have limited knowledge in schools, it is very tough for many students to learn from them. Therefore, for convenience, all section toppers will learn from class toppers that affects the performance of the students.

**Section (SE) level:** A section level is essentially a group of pupils. The top student in a section is the most intelligent and well-versed student in the section compared to the other students. Depending on ranking, the section topper may or may not be the class topper. The section topper will assist in raising pupils' performance levels in that particular area.

**Student Level:** A class in a school is divided into several sections, each of which has a unique group of learners with varying levels of intelligence and learning capacities. Based on their performance in each course, determines their ranking and is further required for the assessment of the class topper, each student is given an equal number of courses. Every student has the chance to raise their score and do better in this situation; nevertheless, if they are unable to do so, their prior score will remain.

**Examination:** A test evaluation known as an examination uses a student's performance index or fitness value to determine how well they done. If

a student does well on an exam, their fitness value will be upgraded; if not, the old result will be kept, and they will have another opportunity to improve their fitness value. Evaluation is done using the best performance index value. In terms of the upcoming exam, student performance increase since class topper learns from section topper as well as section topper learns from students in their specific section, which raises the class topper's Performances index number. Giving the best student in the class is the result (optimal solution).

Learning: The process of learning involves changing one's current conduct and gaining new knowledge. Not all students will necessarily exhibit improved behaviour and perform better, but some will gain new insights and expand their knowledge by studying the section topper.

The section topper in individual class based on learning of the student is expressed as,

$$I^{(S,E+1)} = I_{WF} \times I^{(S,E)} + \quad (18)$$

$$c \times n_2 \times (ST^{(SE,E)} \rho_i - S^{(S,E)} \rho_i) \quad (19)$$

$$S^{(S,E+1)} \rho_i = S^{(S,E)} \rho_i + I^{(S,E+1)}$$

Here, at  $E + 1^{th}$  and  $E^{th}$  examination, the enhancement of student knowledge is denoted as  $I^{(S,E+1)}$  and  $I^{(S,E)}$ , the topper student in section in  $E^{th}$  examination, the performance index is specified as  $ST^{(SE,E)} \rho_i$ . In  $E + 1^{th}$  and  $E^{th}$  examination, the student performance metrics is signified as  $S^{(S,E)} \rho_i$  and  $S^{(S,E+1)} \rho_i$ . The flowchart of CTO is provided in Fig. 6.

Section toppers fight with other section toppers for the title of Class topper, which will enhance their academic performance and learning. Section toppers are the best students in their section. The following equation (21) is derived based on learning of section topper from class topper,

$$I_1^{(SE,E+1)} = I_{WF} \times I_1^{(SE,E)} + C \times n_1 \times \quad (20)$$

$$(CT^{(E)} \rho_i - ST^{(SE,E)} \rho_i) \quad (21)$$

$$ST^{(SE,E+1)} \rho_i = ST^{(SE,E)} \rho_i + I^{(SE,E+1)}$$

Here, the development of knowledge of ST in  $E + 1^{th}$  and  $E^{th}$  examination is represented by  $I_1^{(SE,E+1)}$  and  $I_1^{(SE,E)}$ . Moreover, in  $E^{th}$  examination a class topper performance index is stated as  $CT^{(E)} \rho_i$ . Section topper in  $E + 1^{th}$  and  $E^{th}$  examination performance metrics is signified

as  $ST^{(SE,E)} \rho_i$  and  $ST^{(SE,E+1)} \rho_i$  respectively. Based on this behaviour, the PI controller effectually gets tuned by providing stabilized output with rapid settling time as shown in the Flowchart in Fig. 6. Subsequently, the controlled output is fed to BLDC driven EV through three phase VSI that convert DC-AC, following section explains the modelling of three phase BLDC motor.

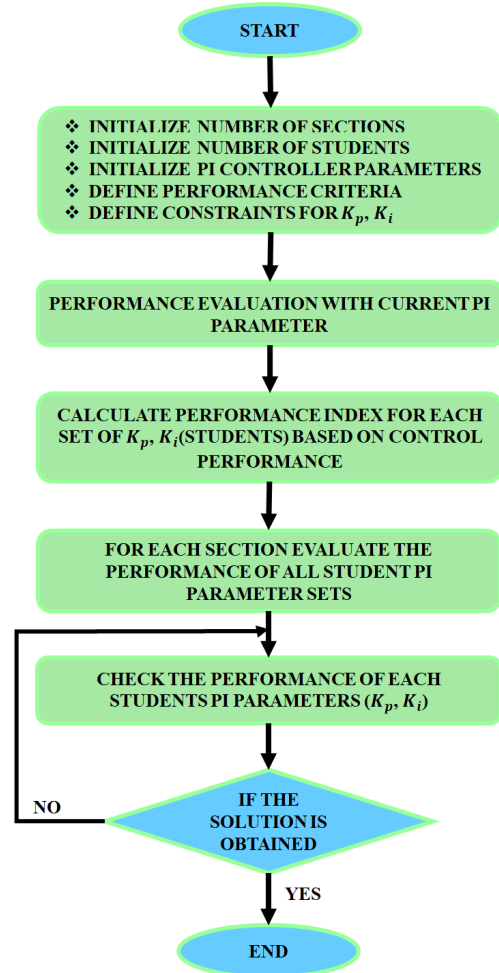


Fig. 6. Flowchart of Class Topper Optimization.

#### D) Modelling of Three Phase BLDC Motor

The BLDC motor is utilized in EVs application as it has the advantage of simple, low cost and maintenance compared to other motors. The three-phase VSI shown in Fig. 7 is used to energize the BLDC motor. Here,  $V_{DC}$  is the voltage across DC link,  $V_{an}, V_{bn}, V_{cn}$  - three phase voltage outcomes. Fig. 7 depicts an equivalent BLDC motor circuit. The BLDC motor, which additionally has symmetrical back trapezoidal EMF coil windings, uses the permanent magnets as its rotor magnet. The rotor current is ignored owing to high resistance value of permanent

magnets. The BLDC motor trained by the way the PM and coil interact.

The BLDC motor voltage equations are expressed as follows,

$$V_a = R_a i_a + \frac{d}{dt} L_a i_a + E_a \quad (22)$$

$$V_b = R_b i_b + \frac{d}{dt} L_b i_b + E_b \quad (23)$$

$$V_c = R_c i_c + \frac{d}{dt} L_c i_c + E_c \quad (24)$$

Here,  $L_a = L_b = L_c = L$  denotes self inductance,  $V_a, V_b, V_c$  specifies per phase stator voltages,  $i_a, i_b, i_c$  specifies per phase stator currents,  $E_a, E_b, E_c$  denotes induced back emf and  $R$  denotes per phase stator resistance correspondingly.

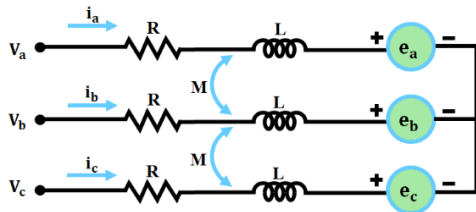


Fig. 7. Equivalent circuit of Three phase BLDC motor.

The expression of the generated back-emf, which has a trapezoidal shape because of the permanent magnet straddling the rotor, is as follows:

$$E_a = K_e * \frac{d}{dt}(\theta) * \omega_r(t) \quad (25)$$

$$E_b = K_e * \frac{d}{dt}(\theta - \frac{2\pi}{3}) * \omega_r(t) \quad (26)$$

$$E_c = K_e * \frac{d}{dt}(\theta + \frac{2\pi}{3}) * \omega_r(t) \quad (27)$$

Here,  $\omega_r$  as well as  $K_e$  states mechanical speed of rotor and back emf constant, consequently, the following equation defined the electromagnetic torque,

$$T_e = \frac{1}{\omega_r} (e_a i_a + e_b i_b + e_c i_c) \quad (28)$$

Subsequently, the speed of this motor has to be regulated, thus PI controller is employed as discussed follows.

E) Modelling of PI Controller For Speed Control

The PI controller is commonly utilised because they are simple to change and tweak, because BLDC motors are multivariate systems, saturation is conceivable. Speed and current are frequently regulated with the use of PI controller. The PI controller as shown in Figure 8, the proportional and integral processes to produce output signal and examines discrepancy between speed feedback signal's real value and its reference value. Following Equation (30) shows the PI controller,

$$y(t) = K_p e(t) + \frac{k_p}{T_i} \int_0^1 e(t) dt \quad (29)$$

Therefore, as seen in Fig. 8, the output signal's state function is  $y(t)$ , whereas regulated input signal's principal function is  $e(t)$ . A time constant, proportionality coefficient  $K_p$ , and integral of time constant  $T_i$  are the three variables that are altered. These parameters are often expressed as coefficients in order to generate the transfer function as indicates below,

$$G(s) = K_p + \frac{ki}{s} \quad (30)$$

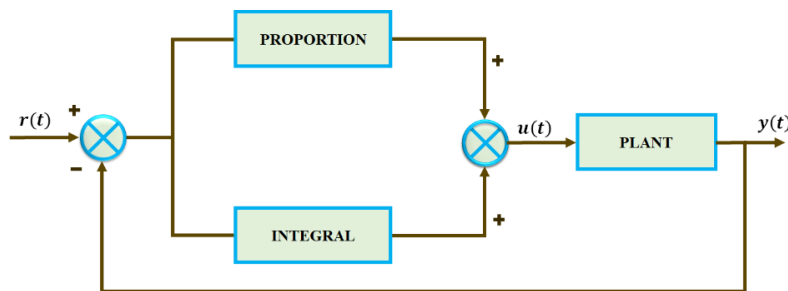


Fig. 8. Schematic configuration of PI controller.

The PI controller Efficiently manage the speed of BLDC motor and lessen torque ripple by solving the of overshoot and stabilization by generating a more dynamic and responsive system. Despite this, the battery storage system is employed for saving surplus energy obtained in PV after delivering adequate power to three phase BLDC motor driven EV. Also, charging and discharging process of battery is handled by bidirectional converter that ensures bidirectional power flow when battery needs to charge, it operates under charging mode and discharge to DC link when battery gets enough supply. Subsequently, in the scenarios of PV module unable to supply BLDC motor, the stored energy in battery supply power back to motor driven EV, thereby power management is attained with high performance.

### III. RESULTS AND DISCUSSION

The overall proposed system is validated through MATLAB/Simulink for showing the significance of converter and optimized PI controller based BLDC motor driven EV. Based on the obtained findings, it is compared with the

recently developed converters and optimization appraoches in terms of efficiency, settling time and convergence speed as dicussed in below. Additionally, proposed system parameter specification is tabulated in Table 2. Fig. 9 denotes the simulation set up of the proposed work.

Table 2

Parameter Specification

| Parameter                        | Specification |
|----------------------------------|---------------|
| <b>PV System</b>                 |               |
| <i>Rated Power</i>               | 10kW          |
| <i>No. of Panels in Parallel</i> | 16            |
| <i>Open Circuit Voltage</i>      | 37.25V        |
| <i>Cell linked in Series</i>     | 36            |
| <i>No. of Panels in series</i>   | 2             |
| <i>Short Circuit Current</i>     | 8.95A         |
| <b>Modified Luo Converter</b>    |               |
| $L_1, L_2, L_3, L_4$             | 4.7mH         |
| <i>Switching frequency</i>       | 10KHz         |
| $C_1, C_2$                       | 22 $\mu$ F    |
| $C_0$                            | 2200 $\mu$ F  |

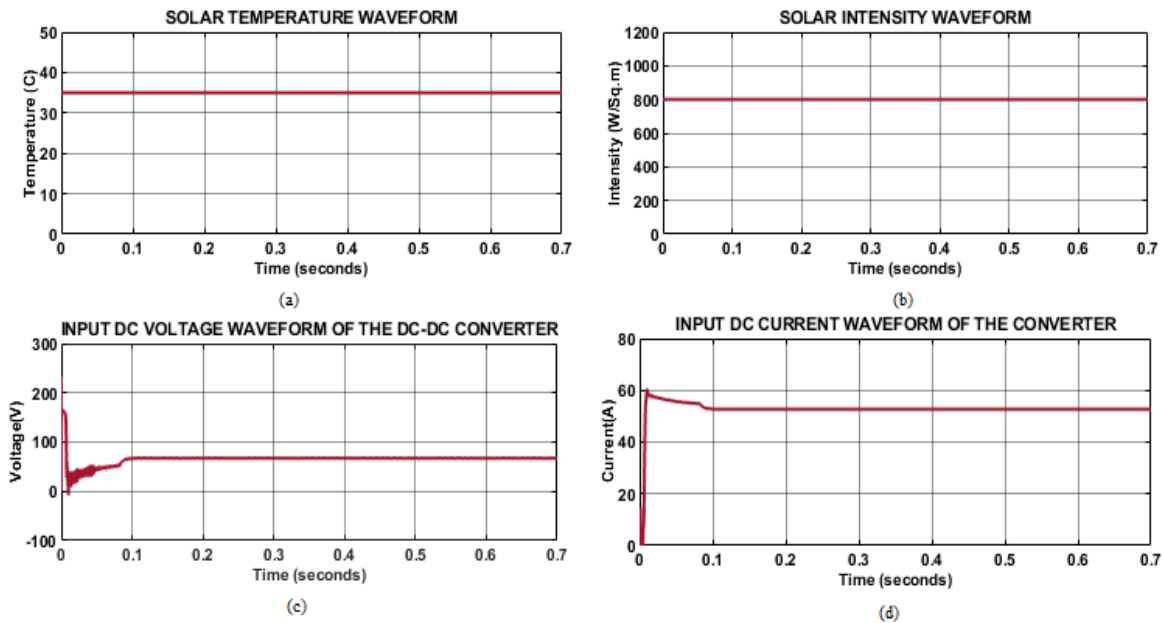
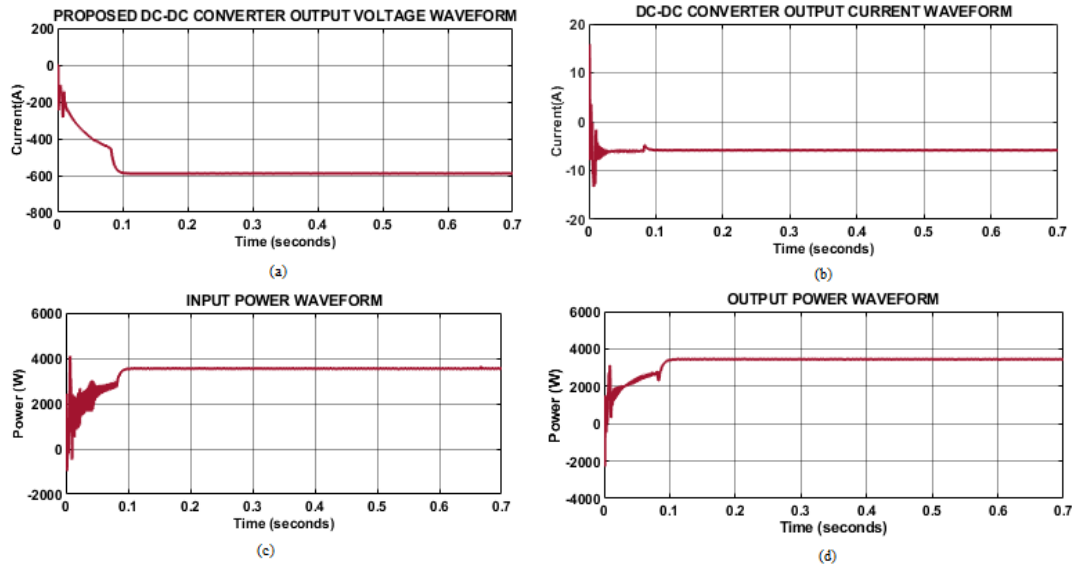


Fig. 9. Solar array Waveforms.

The solar array temperature waveform in Fig. 9(a) specifies that the panel temperature relatively stabilizes at 35°C and the intensity in solar array remains steady at 800(W/Sq.m) as revealed in Fig. 9(b). In Fig. 9(c), output voltage of PV

module gets deviations in starting duration upto 0.1s, after the stable voltage 74V is attained. Similarly, PV output current gets stabilized output at 54A after facing distortions in initial period as represented in Fig. 9(d).



**Fig. 10. Proposed Interleaved Landsman converter waveforms.**

The developed interleaved Landsman converter output voltage waveform indicates that in initial period, voltage gets deviated till 0.1s, after that by utilizing CTO-PI controller the voltage maintained stable at -599V as shown in Fig. 10(a). Subsequently, the output current in Fig. 10(b) signifies that in initial stage, the current oscillated under certain period of time and after

0.1s, it constantly steady at 6.5A. Based on the input and output voltage and current of converter waveforms, power waveforms in Fig. 10(c) indicates that the input power is steadily maintained at 3996W. Similarly, output power also remains continued at 3893W after the time period of 0.1s respectively.

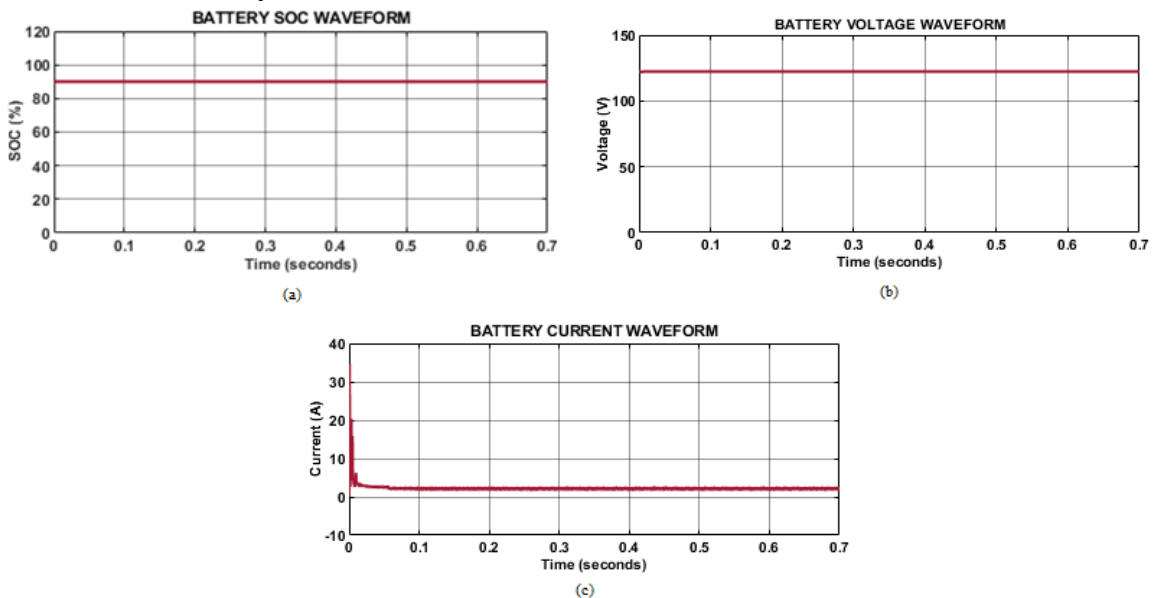


**Fig. 11. Battery Waveforms.**

From Fig. 11(a), which is analysed that battery SoC is constantly maintained at 90% without any deviations. Like, battery voltage waveform in Fig. 11(b) shown, which remains steady at 125V and

battery current is highly oscillated in initial stage and after 0.1s is continued at 3A as signified in Fig. 11(c).

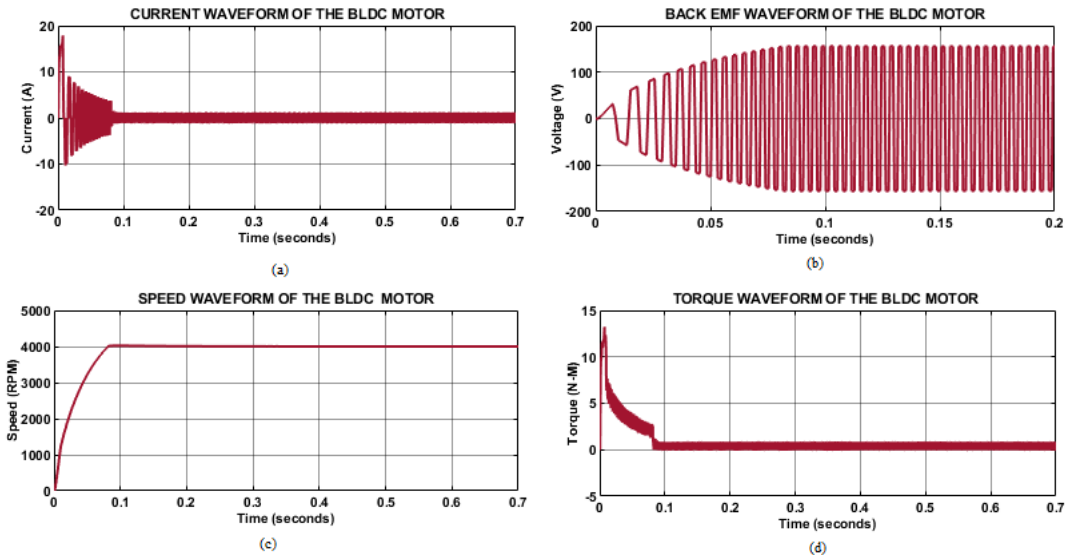


Fig. 12. BLDC motor Waveforms.

The current waveform for the BLDC motor gets highly raised and oscillates upto the time period of 0.1s and gets stabilized output at 3A. Additionally, the back EMF waveform of BLDC motor continually maintains at 180V after the time period of 0.1s as signified in Fig. 12(b). Additionally, speed waveform for BLDC motor represents in Fig. 12(c), which observes that the constant speed is maintained at 4000RPM after the duration of 0.1s respectively. Consequently, Torque waveform in Fig. 12(d) denotes a stabilized output after 0.1s correspondingly.

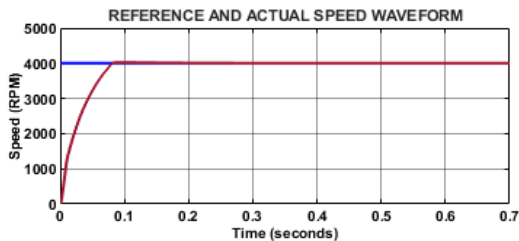


Fig. 13. Reference and Actual Speed Waveform.

The waveform in Fig. 13 shows the performance of a Brushless DC (BLDC) motor. The blue line represents the reference speed, which is set at 4000 RPM. The red line shows how the motor's actual speed changes over time. At the start, the motor quickly accelerates until it reaches the reference speed, by 0.1 seconds, the motor's actual speed has almost reached the desired speed, indicates smooth and efficient speed control.

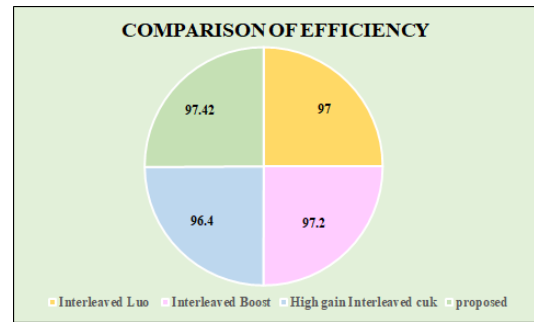


Fig. 14. Comparison of Efficiency.

Comparison of proposed Interleaved Landsman converter is compared with other interleaved converters for foreshowing the significance of designed converter. From Fig. 14, is perceived that the Interleaved Landsman converter accomplishes higher efficiency of 97.42% compared to the other recently developed converters in [21-23].

Table 3

Comparison of Settling time

| Controllers          | Settling time (s) |
|----------------------|-------------------|
| Optimized Fuzzy [24] | 4.0               |
| SSO-PID [25]         | 6.0               |
| FO-PID [26]          | 1.2               |
| Proposed             | 0.1               |

Table 3 Compared the optimized control approaches with proposed CTO-PI controller for finding the better settling time technique, from the table it is shown that proposed optimization based control topology achieves reduced settling time of 0.1s, thereby better stabilized performance is attained for the developed converter.

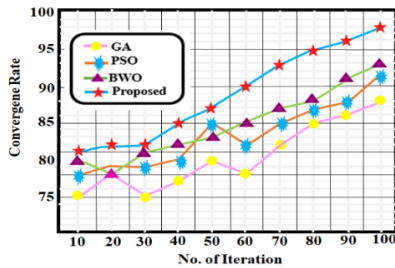


Fig. 15. Comparison of Convergence speed.

The proposed Class Topper optimized PI controller is compared with the other optimization methodologies for convergence speed comparison as illustrated in Fig. 15, which analyzed that by utilizing CTO-PI, the quick convergence speed is accomplished compared to the traditional topologies.

#### IV. CONCLUSION

The proposed research work develops a novel converter with optimization approach for BLDC motor driven EV applications. With the aid of designed Interleaved Landsman converter, improved power handling with higher conversion efficiency is delivered to the BLDC motor. Additionally, Class topper Optimization approach effectively performs well by tuning the parameters of PI with rapid settling time and convergence speed, thereby enhancing stability. The battery system with bidirectional converter ensures energy management by adequately supplying energy to BLDC motor during peak times. Also, the BLDC motor gets proficiently regulated with the help of PI controller, which making the motor operating at desired speed. Overall, the MATLAB/Simulink outcomes demonstrates higher voltage conversion efficiency of 97.42% with rapid settling time of (0.1s) and convergence speed compared to the other conventional approaches as analyzed in the comparative analysis. These findings establish the potential of this system to revolutionize EV propulsion by providing an energy-efficient, scalable and sustainable solution, supporting the broader adoption of renewable energy-driven EV technologies. The proposed concept is validated only through simulation and hence the future work will concentrate on developing a hardware prototype for validating the performance of the system experimentally under real-world operating conditions.

#### References

[1] Saiteja P., Ashok B., Mason B., Kumar P.S. Assessment of Adaptive Self-Learning-Based BLDC Motor Energy Management Controller in

Electric Vehicles Under Real-World Driving Conditions for Performance Characteristics. *IEEE Access*, 2024.

[2] Chanana I., Sharma A., Kumar P., Kumar L., Kulshreshtha S., Kumar S., Patel S.K. Combustion and stubble burning: A major concern for the environment and Human Health. *Fire*, 2023, vol. 6, no. 2, pp. 79.

[3] Kavin, K. S., Subha Karuvelam P., Devesh Raj M., Sivasubramanian M. A Novel KSK Converter with Machine Learning MPPT for PV Applications. *Electric Power Components and Systems*, 2024, pp. 1-19.

[4] Subbarao M., Dasari K., Duvvuri S.S., Prasad K.R., Narendra B.K., Krishna V.M. Design, control and performance comparison of PI and ANFIS controllers for BLDC motor driven electric vehicles. *Measurement: Sensors*, 2024, vol. 31, pp. 101001.

[5] Madichetty S., Mishra S., Basu M. New trends in electric motors and selection for electric vehicle propulsion systems. *IET Electrical Systems in Transportation*, 2021, vol. 11, no. 3, pp. 186-199.

[6] Radhakrishnan R.K., Marimuthu U., Balachandran P.K., Shukry A.M., Senjyu T. An intensified marine predator algorithm (MPA) for designing a solar-powered BLDC motor used in EV systems. *Sustainability*, 2022, vol. 14, no. 21, pp. 14120.

[7] Akshaya P., Joyslin Janet J., Mohana Indhu Priya A., Anusuya Devi G., Karthik Kumar K., Kamaraja A.S. Steady state and dynamic performance investigation of solar interlinking BLDC motor for electric vehicle application. In *2021 Second International Conference on Electronics and Sustainable Communication Systems (ICESC)*, 2021, pp. 63-68. IEEE.

[8] Cheruku R., Kim J.H., Krishna V.M., Periyat P., SSSR S.D. Photo-electrodes decorated with carbon quantum dots: Efficient dye-sensitized solar cells. *Results in Engineering*, 2023, vol. 20, pp. 101611.

[9] Pires V.F., Cordeiro A., Foito D., Silva J.F. Dual output and high voltage gain DC-DC converter for PV and fuel cell generators connected to DC bipolar microgrids. *IEEE Access*, 2021, vol. 9, pp. 157124-157133.

[10] Imanlou A., Behkam R., Nadermohammadi A., Nafisi H., Heydari-Doostabad H., Gharehpetian G.B. A New High Voltage Gain Transformer-Less Step-Up DC-DC Converter with Double Duty-Cycles: Design and Analysis. *IEEE Access*, 2024.

[11] Gholizadeh H., Gorji S.A., Afjei E., Sera D. Design and implementation of a new cuk-based step-up DC-DC converter. *Energies*, 2021, vol. 14, no. 21, pp. 6975.

[12] Prabhu P., Urundady V. Design of coupled inductors using split winding scheme for bridgeless SEPIC. *IET Power Electronics*, 2020, vol. 13, no. 7, pp. 1434-1444.

- [13] Rezvanyvardom M., Mirzaei A., Shabani M., Mekhilef S., Rawa M., Wahyudie A., Ahmed M. Interleaved step-up soft-switching DC–DC Boost converter without auxiliary switches. *Energy Reports*, 2022, vol. 8, pp. 6499-6511.
- [14] Khorasani R.R., Jazi H.M., Chaudhuri N.R., Khoshkbar-Sadigh A., Shaneh M., Adib E., Wheeler P. An interleaved soft switched high step-up boost converter with high power density for renewable energy applications. *IEEE Transactions on Power Electronics*, 2022, vol. 37, no. 11, pp. 13782-13798.
- [15] Gui Y., Han R., Guerrero J.M., Vasquez J.C., Wei B., Kim W. Large-signal stability improvement of DC-DC converters in DC microgrid. *IEEE Transactions on Energy Conversion*, 2021, vol. 36, no. 3, pp. 2534-2544.
- [16] Debdouche N., Zarour L., Chebabhi A., Bessous N., Benbouhenni H., Colak I. Genetic algorithm-super-twisting technique for grid-connected PV system associate with filter. *Energy Reports*, 2023, vol. 10, pp. 4231-4252.
- [17] Roslan M.F., Al-Shetwi A.Q., Hannan M.A., Ker P.J., Zuhdi A.W. Particle swarm optimization algorithm-based PI inverter controller for a grid-connected PV system. *PloS one*, 2020, vol. 15, no. 12, pp. e0243581.
- [18] Goswami A., Sadhu P.K. Stochastic firefly algorithm enabled fast charging of solar hybrid electric vehicles. *Ain Shams Engineering Journal*, 2021, vol. 12, no. 1, pp. 529-539.
- [19] Premkumar K., Vishnupriya M., Sudhakar Babu T., Manikandan B.V., Thamizhselvan T., Nazar Ali A., Rabiul Islam M., Kouzani A.Z., Parvez Mahmud M.A. Black widow optimization-based optimal PI-controlled wind turbine emulator. *Sustainability*, 2020, vol. 12, no. 24, pp. 10357.
- [20] Shubham, Roy S.P., Mehta R.K., Singh A.K., Roy O.P. A novel application of jellyfish search optimisation tuned dual-stage (1+ PI) TID controller for microgrid employing electric vehicle. *International Journal of Ambient Energy*, 2022, vol. 43, no. 1, pp. 8408-8427.
- [21] Jegha A.D., Subathra M.S., Kumar N.M., Ghosh A. Optimally tuned interleaved Luo converter for PV array fed BLDC motor driven centrifugal pumps using whale optimization algorithm—A resilient solution for powering agricultural loads. *Electronics*, 2020, vol. 9, no. 9, pp. 1445.
- [22] Akhlaghi B., Farzanehfard H. Efficient ZVT cell for interleaved DC–DC converters. *IET Power Electronics*, 2020, vol. 13, no. 10, pp. 1925-1933.
- [23] Shyma H., Sebastian E., Thomas R.P. High Gain Interleaved Cuk Converter with Phase Shifted PWM. *International Journal of Engineering & Science*, 2016, vol. 5, no. 8, pp. 27-32.
- [24] Jain A., Sharma A., Jatley V., Azzopardi B., Choudhury S. Real-time swing-up control of non-linear inverted pendulum using Lyapunov based optimized fuzzy logic control. *IEEE Access*, 2021, vol. 9, pp. 50715-50726.
- [25] Khan H., Khatoon S., Gaur P., Abbas M., Saleel C.A., Khan SA. Speed control of wheeled mobile robot by nature-inspired social spider algorithm-based PID controller. *Processes*, 2023, vol. 11, no. 4, pp. 1202.
- [26] Saleem A., Soliman H., Al-Ratrouf S., Mesbah M. Design of a fractional order PID controller with application to an induction motor drive. *Turkish Journal of Electrical Engineering and Computer Sciences*, 2018, vol. 26, no. 5, pp. 2768-2778.

#### Information about authors.



**Vendoti Suresh** is working at Godavari Institute of Engineering and Technology, India. His main area of interest includes Renewable Energy Sources and Smart Grid. Email: [sureshvendoti.phd@gmail.com](mailto:sureshvendoti.phd@gmail.com)



**Dondapati Ravi Kishore** is working at Godavari Global University, Rajahmundry. His main area of interest includes Power systems, Renewable Energy Systems, and Energy Auditing. Email: [dravikishore@gmail.com](mailto:dravikishore@gmail.com)



**Gorrupotu Veera Jahnvi** studying at Godavari Institute of Engineering and Technology. Her area of interests includes Renewable Energy Sources. Email: [veerajahnavigorrupotu@gmail.com](mailto:veerajahnavigorrupotu@gmail.com)



**Dulam Manjula** studying in department of Electrical and Electronics Engineering in Godavari Institute of Engineering and Technology from Jawaharlal Nehru Technological University, Kakinada. Her area of interests includes Power Electronics. Email: [manjuladulam14@gmail.com](mailto:manjuladulam14@gmail.com)



**Manne Lokesh** studying at Godavari Institute of Engineering and Technology from Jawaharlal Nehru Technological University, Kakinada. His area of interests includes Smart grids. Email: [manne.lokesh365@gmail.com](mailto:manne.lokesh365@gmail.com)